SUPPLEMENTARY INFORMATION

Intraoperative Detection of Liver Tumors Aided by Fluorescence Goggle System and Multimodal Imaging

Yang Liu[a,b], Walter Akers[a], Adam Q. Bauer[a], Suman Mondal[a], Kyle Gullicksrud[a], Gail Sudlow[a], Joseph P. Culver[a,b], Samuel Achilefu[a,b,c,*]

Departments of [a]Radiology, [b]Biomedical Engineering, and [c]Biochemistry & Molecular Biophysics, Washington University, St. Louis, MO 63110, USA

1. **Fluorescence Goggle System.**

The configuration of goggle system was similar to the previously reported system, except for the NIR light source[1]. Briefly, the detector was developed from a CCD camera (iGEN NV20/20-IC, First Texas Products, El Paso, TX, USA). A long pass filter (820 nm; #8480, Omega Optical, Brattleboro, VT, USA) was used as emission filter. The NIR light source consisted of four high-power LEDs (#H2A1-H760, Roithner Lasertechnik, Vienna, Austria). A short pass filter (775 nm; #NT64-615, Edmund Optics, Barrington, NJ, USA) was employed as emission filter.

2. NIR Contrast Agent.

FDA-approved contrast agent indocyanine green was purchased from Sigma-Adrich (St. Louis, MO, USA). This dye has absorption and emission maxima around 780nm and 830 nm, respectively, in biological media.

3. Mouse Breast Cancer Liver Metastases Model and Fluorescence-guided Liver Surgery.

All animal procedures were conducted in compliance with Washington University Animal Studies Committee's requirements for the care and use of animals in research. For breast cancer liver metastases model, male 4-week old BALB/c mice were purchased from Taconic Farms (Hudson, NY, USA). Mice were anesthetized with ketamine (80 mg/kg) and xylazine (13 mg/kg) cocktail injected intraperitoneally (IP). A 2-mm midline incision was made in the epigastric region to expose the liver. 4T1*luc* cells (100,000) were subsequently implanted into the liver through 27 gauge needle followed by gentle pressure for 1 minute to prevent backflow of cells.

The growth of liver metastases was monitored using bioluminescence imaging. Approximately 4 weeks after cell injection, image-guided liver resections were performed.

For the fluorescence-guided liver resection, mice were anesthetized as above. The hair overlaying the region of interest was removed by gentle clipping and cream depilatory (Sally Hansen, Morris Plains, NJ, USA). ICG solution (0.5mg/kg body weight ICG in saline) was injected intravenously via lateral tail vein. 48 hours after injection (Group1) or 24 hours after injection (Group 2), a midline incision was made from xyphoid to pubis and the liver exposed. The liver was first examined by visual inspection and palpation without the aid of fluorescence guidance. This was followed by re-inspection of the liver using the goggle system. The fluorescence goggle is considered an instrument with "nonsignificant risk" because it neither has a direct contact with patients nor uses ionizing radiation. In this study, the light source was upgraded from two 770 nm LEDs to four high-power 760 nm LEDs. In contrast to regular LEDs that are typically driven by tenths of mA current, the high power LEDs can be driven by hundreds of mA current. With significantly increased forward current, each high power LED generates more photons for the fluorophore excitation than regular LEDs, thereby enhancing NIR fluorescence in the tumors. The high power LEDs can be driven by four consecutive settings of forward bias current settings to provide different levels of NIR excitation (up to 1.49 mW/cm^2 in irradiance at 0.5 m working distance) as needed. The intraoperative imaging of mice was conducted with the fluorescence goggle operating at video rate (30 frames per second). The liver tumors highlighted by fluorescence signal were imaged and displayed in the goggle eyepiece in real time. The emission/excitation filter pairs (775nm short pass/820 nm long pass) provided effective way to image fluorescence with minimal background due to crosstalk. Noticeable motion artifacts were not observed owing to the video-rate imaging capability of the fluorescence goggle. The point-of-view was synchronized with the wearer's head movements, and the orientation of objects within the field of view aligned with that of human vision. Unlike stationary devices, the fluorescence goggle system is a wearable system. Therefore, the working distance slightly changed with the wearer's postures. The average working distance was approximately 0.5 m. The goggle system was fully battery-operated, minimizing the need for external power source during surgery and simplifying the workflow. The data were transferred in real time to a remote computer for storage and further analysis. Tumor positions, extensions, and potential presence of small lesions were assessed based on the fluorescence information obtained from the goggle system. Differences between goggle-aided and unaided observations were noted. Tissues with high fluorescence signal were resected under fluorescence guidance. Surgical sites were then re-examined by visual inspection and fluorescence guidance to explore the presence of residual cancerous tissues and small tumor nodules, which were collected. The mice were euthanized immediately after experiments by cervical dislocation while still under anesthesia. Resected tissues were examined *ex vivo* to compare fluorescence in cancerous versus non-cancerous tissue.

Tissues were subsequently embedded with Tissue-Tek OCT (Sakura Finetek, Torrance, CA, USA) and frozen for histology.

4. Rabbit Liver Cancer Model and Liver Surgery under Multimodal Detection Scheme.

6 week old New Zealand White rabbits were purchased from Taconic Farms (Hudson, NY, USA). Small VX2 tumor tissue fragments were graciously provided by Dr. Gregory Lanza. Before liver tumor implantation, the rabbits were anesthetized with a cocktail of acepromazine (2.5 mg/kg) and ketamine hydrochloride (44 mg/kg) administered through intramuscular injection. Sodium pentobarbital were supplied to the rabbits i.v. via a marginal ear vein to maintain anesthesia. We shaved and prepped the abdomen using aseptic technique. Under the guidance of ultrasound, small VX2 tumor segments were implanted into the liver using a 13 gauge trocar needle preloaded with gel foam for coagulation (Supplementary Figure 3).

Approximately 14 days after implantation, hepatectomy under multimodal image guidance was performed under general anesthesia and with aseptic operative technique. ICG solution (0.5mg/kg body weight ICG in saline) was injected intravenously 48 hours before the surgery. A midline incision from xyphoid to umbilicus was performed, and the falciform and left triangular ligaments were divided to free the right and left lateral lobe of the liver. The liver was examined with ultrasonic imaging and goggle-aided NIR fluorescence imaging to locate the liver tumors. A hepatic resection was performed under the fluorescence guidance. After resection, the surgical bed was re-examined using the fluorescence goggle. The rabbits were sacrificed immediately after hepatectomy.

5. Histology and Microscopy. Resected cancerous tissues and control liver tissues were frozen in OCT. The tissues were sectioned in the cryostat to 8 μm thickness. For fluorescence microscopy, slides were taken directly from the -80 ºC freezer to the Olympus BX51 upright epifluorescence microscope (Olympus America, Center Valley, PA, USA). NIR (775+/-50 nm excitation, 810 nm longpass dichroic, and 845+/-55 nm emission filters) and brightfield images were acquired and merged to create composite images in ImageJ. The same slides were then stained with hematoxylin and eosin (H&E). Matching regions with fluorescence microscopy were identified and imaged.

6. Statistical Analysis

Graphs were generated and statistical analysis was performed with Graphpad Prism. Fluorescence values were reported as mean and standard deviation. To test difference in

fluorescence between lesions and surrounding tissues, Student's t-test was performed and p value was calculated with the Graphpad Prism software.

Supplementary Figures

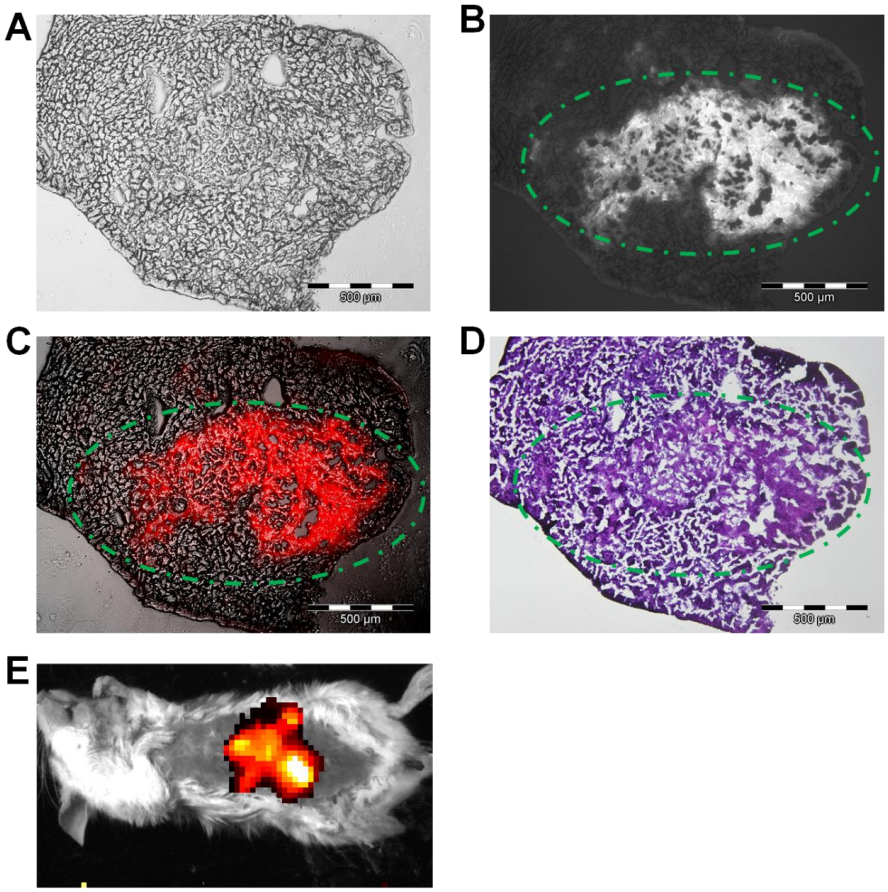

Supplementary Figure 1: Histology and bioluminescence imaging of liver metastases. **(A-D)** are fluorescence and color microscopy of breast cancer liver metastases resected under fluorescence-guidance. **(A)** white light microscopy, (**B)** Fluorescence microscopy ((775ex/810em), **(C)** composite image of fluorescence and white light microscopy, and **(D)** color microscopy after H&E staining of the same section from the mouse model are shown. ICG accumulate in a small metastasis of approximately 1mm in diameter. The liver metastasis exhibits higher fluorescence level than surrounding liver tissues. The contour of ICG fluorescence matches well with that of cancerous tissue manifested by H&E staining. On the H&E image, the metastasis is different from surrounding liver tissues, evident by the epithelial inclusion. Green dashed lines outline cancerous tissues. **(E)** Composite image of bioluminescence image (integration time: 5 mins) and white light image of a mouse. The presence of cancer in the liver was confirmed.

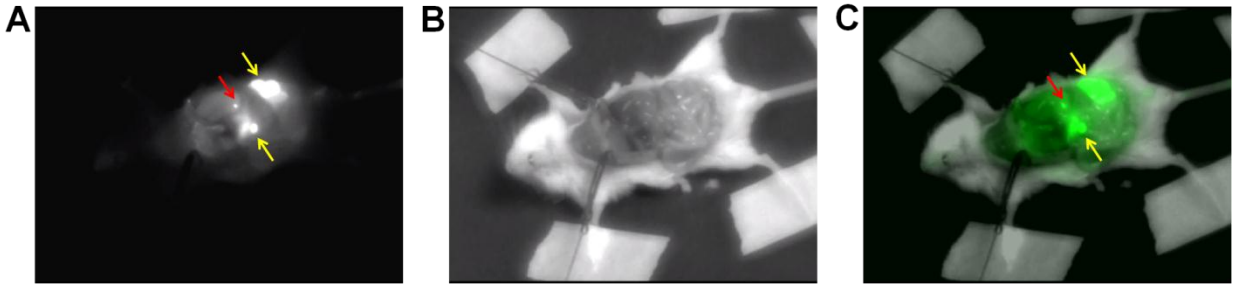

Supplementary Figure 2: Detection of breast cancer liver metastases with fluorescence goggle and ICG was achieved in 2 mice in Group 2. Intraoperative (A) NIR fluorescence image, (B) reflectance image and (C) merged image of (A) and (B) of a mouse 24 hours post-injection of ICG are shown. Fluorescence goggle detects a metastasis in the liver intraoperatively. NIR fluorescence is pseudo-colored in green in (C). Red arrows indicate the metastasis, and yellow arrows indicate the intestines. In this mouse, the metastasis and intestines have higher fluorescence signal than the liver.

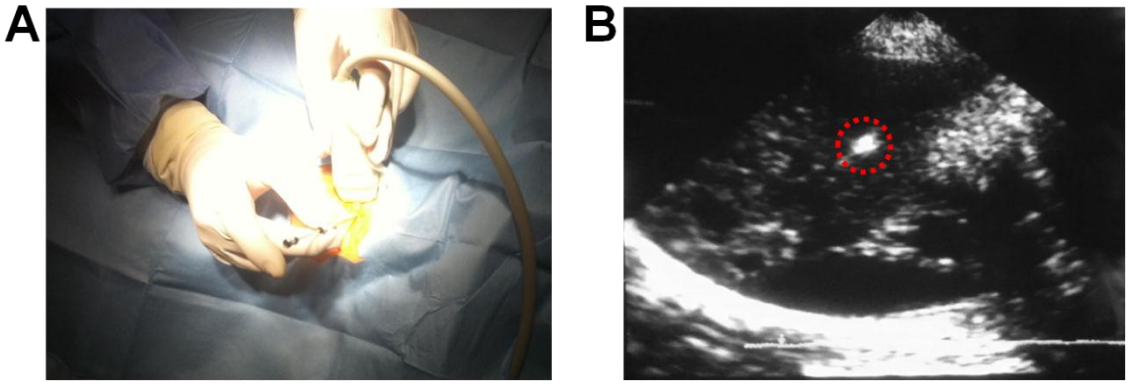

Supplementary Figure 3: Minimally-invasive liver tumor implantation in rabbits. Ultrasound-guided tumor implantation using a trocar needle. (A) photo of surgical procedure; (B) ultrasonic image immediately after implantation, where implantation site is highlighted with red circle. The implantation site is hyperechoic because of the high water content in the tumor segments and gel foam.

References:

1. Y. Liu, A. Q. Bauer, W. J. Akers, G. Sudlow, K. Liang, D. Shen, M. Y. Berezin, J. P. Culver and S. Achilefu, *Surgery*, **149**, 689-698.